

## Chapter 5

# COMPUTER SIMULATIONS OF PHASE TRANSITIONS IN LIQUID CRYSTALS

D. FRENKEL

### 1. Introduction

The aim of these lectures is twofold. First, I wish to give a simple introduction to the computer simulations of classical many-body systems, with special emphasis on those technical aspects that are of particular relevance for simulation of liquid crystals.

To this end, I first give a brief elementary introduction to Molecular Dynamics and Monte Carlo simulations of classical many-body systems. Thereupon (section 4) I discuss the choice of technique and simulation ensemble. Section 5 deals with 'measurements' in a computer simulation. In Section 6, techniques to locate first order phase transitions are discussed. In this context, a brief discussion of free energy calculations is included. This 'technical' introduction is quite sketchy. The material presented in this Chapter is based on articles that have been published elsewhere. For a more detailed discussion, the reader is referred to one of the many excellent textbooks on this topic, e.g. the book of Allen and Tildesley<sup>1</sup>.

Next, we apply the tools that we have thus introduced to computer simulation of simple models that exhibit liquid-crystalline behavior. In particular, I shall discuss computer-simulation studies of simple models that exhibit nematic, smectic and columnar phases. The isotropic-nematic transition in two-dimensions is rather different from its 3D counterpart and is therefore discussed separately. I conclude with a discussion of recent developments and their possible implications for the numerical study of liquid-crystalline phases and phase transitions.

### 2. Monte Carlo Simulation

The prime purpose of the kind of Monte Carlo or Molecular Dynamics simulations that we shall be discussing, is to compute equilibrium properties of classical many-body systems. Let us first look at Monte Carlo (MC) simulations. Such simulations are used to compute ensemble averaged static properties of classical many-body systems. In the canonical (i.e. constant-NVT) ensemble, the ensemble average of a function  $A(q^N)$  of the particle coordinates  $\{q^N\}$  is defined as:

---

D. Frenkel - FOM Institute for Atomic and Molecular Physics, Kruislaan 407, 1098 SJ Amsterdam, The Netherlands.

*Phase Transitions in Liquid Crystals*, Edited by S. Martellucci and A.N. Chester, Plenum Press, New York, 1992

$$\langle A \rangle_{NVT} = \frac{\int dq^N A(q^N) \exp(-\beta U(q^N))}{\int dq^N \exp(-\beta U(q^N))} \quad (1)$$

In Eq. 1,  $\beta = 1/k_B T$  (where  $T$  is the absolute temperature and  $k_B$  the Boltzmann constant), and  $U(q^N)$  is the potential energy function. In the Metropolis Monte Carlo method,  $\langle A \rangle$  is estimated as the *unweighted* average of the values  $A(q^N)$  sampled during a random walk through configuration space. The trick of the Metropolis MC method is to construct this random walk in such a way that the probability to visit a particular point  $q^N$  is proportional to the Boltzmann factor  $\exp(-\beta U(q^N))$ . There are many ways to construct such a random walk. In the approach proposed by Metropolis et al.<sup>2</sup> the construction of a step in the random walk consists of two steps. First a random trial move is made from the current position in configuration-space  $q^N$  to a trial position  $q'^N$ . Usually, such a trial move corresponds to the displacement of a single particle. But other moves are acceptable, as long as the probability of attempting a move from  $q^N$  to  $q'^N$  is equal to the probability of a trial move from  $q'^N$  to  $q^N$ . Whether or not a trial move is in fact accepted depends on the change in potential energy,  $\Delta U$ , associated with the trial move. If  $\Delta U < 0$ , the move is always accepted. If  $\Delta U > 0$ , the move is accepted with a probability  $\exp(-\beta \Delta U)$ , and rejected otherwise. The quantity  $A$  is computed at the position that results after accepting or rejecting the trial move. The average of all these 'measurements' of  $A$  during the random walk yields the desired ensemble average  $\langle A \rangle_{NVT}$ .

### 2.1. Periodic boundary conditions

For a system with short-range forces, the precise nature of the boundary conditions should be unimportant in the thermodynamic limit. The problem is that the number of particles in a normal simulation is of the order of  $10^2$  to  $10^3$ . If *real* boundaries are used in a simulation (e.g. hard walls), then the particles at the boundaries experience interactions very different from those in the bulk. This results in a correction to all equilibrium properties. Sure enough, such a correction would vanish in the thermodynamic limit, but only as  $N^{-(1/D)}$ , where  $D$  is the dimensionality of the system. In contrast, periodic boundary conditions mimic the situation where the system is embedded in an infinite, homogeneous sample of the same phase. There are still system-size effects, but these are much weaker (e.g. of order  $N^{-1}$  or  $(\ln N)/N$ ). In a 3D simulation, one should also consider the shape of the simulation box. For simulations on liquids, a cubic shape is simplest, and in most cases perfectly adequate. For the perfectionist, other shapes are sometimes preferable (see Ref. 1).

In contrast, for crystalline solids and smectic or columnar liquid crystals, the choice of the shape of the unit box is not simply a matter of taste. It is clearly essential that the simulation box be commensurate with the periodicity of the ordered phase. For highly symmetric solid phases this is easy to achieve. However, for phases with lower than cubic symmetry, the shape of the unit-cell of the crystal depends on temperature and pressure, and this dependence is not known *a priori*. The most extreme example of such a dependence is a phase transition from one solid phase to another. At such a transition, the crystal unit cell may take on a completely different shape. If the simulation box cannot adapt to the new structure, such a phase transition would be artificially suppressed. A Molecular Dynamics technique that overcomes this problem was introduced in 1980 by Parrinello and Rahman<sup>3,4</sup>. The Parrinello-Rahman technique can easily be incorporated in a Monte Carlo program<sup>5</sup>.

So much for the good news. Now some of the problems. In small systems, periodic boundary conditions may not be quite as harmless as they seem. They may induce artificial cubic order in

a system that would otherwise be isotropic. Usually this induced order has only a minor effect on 'scalar' properties of atomic fluids (such as the energy or the pressure). However, it may have a pronounced effect on the tensor properties of atomic fluids, in particular those that depend on correlations between three or more atoms<sup>6,7</sup>. In molecular fluids the periodic boundaries may influence the orientational distribution function of the molecules, and thereby all properties that depend on this quantity<sup>8</sup>. Obviously, this effect of periodic boundaries is of considerable relevance for the numerical study of liquid crystals.

## 2.2. Intermolecular Interactions

Selecting the most convenient form for the intermolecular interactions to be used in a simulation is an art in itself. On this topic, I will limit myself to a few general remarks. The first may be superfluous, but I believe that it cannot be said too often. There is a fundamental distinction between simulations that aim to model *real* substances, and those that focus on testing theoretical concepts. For the latter kind of simulation it is essential to use the simplest possible interaction potential that reproduces the essential physics of the problem. Any more complicated potential just makes comparison with theory harder and the simulation slower. In contrast, if the aim is to understand the behaviour of real systems, then it is advisable to use the best potential energy function that you can get. Again, the reason is simple. If you are not using the best potential and you find that simulation and experiment are at odds then *you have learned nothing*. But if you use the best available potential, then a discrepancy between simulation and experiment is meaningful. Often, the nature of the discrepancy suggests how to improve the potential function.

## 2.3. Monte Carlo Moves and Myths

Monte Carlo trial moves should be generated in such a way that, in the absence of the Boltzmann factors, the probability to go from point  $\alpha$  to point  $\beta$  in configuration space should be equal to the probability to return from  $\beta$  to  $\alpha$ . For translational moves (i.e. displacements of the center-of-mass of a molecule) this condition is so easy to satisfy that it almost requires an effort to get it wrong. However, for orientational moves, the choice of the random displacement requires a little more care: it is only too easy to generate orientational moves that lead to a distortion of the orientational distribution function of the molecules. This point is discussed in detail in Ref. 1. It is clearly of crucial importance for the numerical study of liquid crystals that the sampling scheme does not bias the orientational distribution function. In the case of large flexible molecules with constraints on some bondlengths and bondangles it is still possible to perform Monte Carlo sampling of the internal degrees-of-freedom<sup>9</sup>. However, for such model systems the conventional Monte Carlo sampling becomes very cumbersome and other schemes are needed to perform efficient numerical simulations. I will return to this point later.

How large should a Monte Carlo trial move be? If it is very large, it is likely that the resulting configuration will have a high energy and the trial move will probably be rejected. If it is very small, the change in potential energy is probably small and most moves will be accepted. In the literature one often finds the mysterious state that an acceptance of approximately 50 % should be optimal. This statement is not always true. For a rational discussion of the acceptance criterion it is necessary to state what exactly is meant by 'optimal'.

My preferred definition of 'optimal' is as follows: *That Monte Carlo sampling scheme is optimal, which yields the lowest statistical error in the quantity to be computed for a given expenditure of 'computing budget'*. Usually, 'computing budget' is equivalent to CPU time. From this definition it is clear that, in principle, a sampling scheme may be optimal for one

quantity but not for another. Actually, the above definition is all but useless in practice (as are most definitions). It is just not worth the effort to measure the error estimate in, for instance, the pressure, as a function of the Monte Carlo step-size for a series of runs of fixed length. However, it is reasonable to assume that the meansquare error in the 'observables' is inversely proportional to the number of 'uncorrelated' configurations visited in a given amount of CPU time. And the number of independent configurations visited is a measure of the distance covered in configuration space. This suggests a more manageable criterion to estimate the efficiency of a Monte Carlo sampling scheme, namely, the sum of the squares of all displacements in configuration space divided by computing time. This quantity should be distinguished from the meansquare displacement per unit of computing time, because the latter quantity goes to zero in the absence of diffusion, whereas the former does not.

If we try to translate the present criterion into a rule for the optimal acceptance ratio, it is easy to see that different Monte Carlo codes will have different optima. The reason is that it makes a crucial difference if the amount of computing required to test whether a trial move is accepted depends on the magnitude of the move. More generally, for continuous potentials where *all* interactions have to be computed before a move can be accepted or rejected, the amount of computation does not depend on the size of a trial move. However, the situation is very different for simulations of molecules with a hard repulsive cores. Here a move can be rejected as soon as overlap with *any* neighbor is detected. In this case, a rejected move is cheaper than an accepted one, and hence the average computing time per trial move goes down as the step-size is increased. As a result, the optimal acceptance ratio for hard-core systems is appreciably lower than for systems with continuous interactions. Exactly how much depends on the nature of the program, in particular on whether it is a scalar or a vector code (in the latter case hard-core systems are treated much like continuous systems), how the information about neighbor-lists is stored, and even on the computational 'cost' of random numbers and exponentiation. The consensus seems to be that for hardcore systems the optimum acceptance ratio is closer to 20 % than to 50 %, but this is just another rule-of-thumb. As computers and models change, old rules-of-thumb may have to change too.

### 3. Molecular Dynamics

The structure of a Molecular Dynamics program differs only little from that of a Monte Carlo program, yet the two approaches are very different. In a Monte Carlo simulation equilibrium averages are estimated by sampling an integral over configuration space, such as in Eq. 1. The result of such a simulation is an estimate of the ensemble-average of the quantity of interest. The order in which points in configuration space are sampled has no physical meaning, and hence a Monte Carlo simulation yields no dynamical information. In contrast, a Molecular Dynamics simulation follows the natural time-evolution of a classical many-body system along its path in phase space. Molecular Dynamics simulations yield time-averages rather than ensemble-averages. An important consequence of this fact is that the method can be used to measure time-dependent quantities (e.g. time-correlation functions). This last feature of Molecular Dynamics, combined with the fact that an MD program is as simple as an MC program, is responsible for the fact that the majority of all simulations on classical many-body systems employ MD rather than MC. Nevertheless, there are situations where MC is more convenient. The choice of technique will be discussed in Section 4. In the present section, I present a very elementary description of the Molecular Dynamics method.

### 3.1. Algorithm

In a Molecular Dynamics program, the time-evolution of a classical many-body system is simulated by numerical integration of Newton's equations of motion. The central part of any MD program is therefore the algorithm to carry out this integration. However, it should be stressed that the actual time spent on integrating the equations of motion is negligible compared with the time it takes to compute all intermolecular forces.

A large number of algorithms exist that can be used to integrate the equations of motion of systems of particles with continuous intermolecular forces. These algorithms integrate the equations of motion using a finite difference method. Clearly, it is important to choose the best available algorithm. In order to do so, it is necessary to specify what we mean by a 'good' algorithm. There are several criteria that a good algorithm should satisfy. For the sake of comparison, we assume that all algorithms can be made to do an equally good job in reproducing the trajectory of the system through phase-space, and that they keep all 'conserved' quantities (e.g. energy, total momentum) constant to the same degree of accuracy. The comparison which then remains is simply: which algorithm is cheapest. As before, what is 'expensive' on one computer (e.g. memory) may be 'cheap' on another.

The idea behind many of the more sophisticated algorithms is that it is possible to use a larger integration step (and thereby to gain in speed), by utilizing stored information about the higher derivatives of the particle-coordinates. Although this is certainly true in principle, it turns out that, unless very high accuracy is needed, the very simplest MD algorithm, named after Verlet<sup>10</sup>, is as good as most higher-order schemes<sup>11</sup>. The Verlet algorithm can be derived in the following way. First, we express the positions of a particle at times  $t + \Delta t$  and  $t - \Delta t$  in terms of its position, velocity and acceleration at time  $t$ :

$$\begin{aligned} x(t + \Delta t) &= x(t) + \dot{x}\Delta t + \frac{1}{2}\ddot{x}\Delta t^2 + \dots \\ x(t - \Delta t) &= x(t) - \dot{x}\Delta t + \frac{1}{2}\ddot{x}\Delta t^2 + \dots \end{aligned} \quad (2)$$

Adding these two equations, and subtracting  $x(t - \Delta t)$  from both sides, yields:

$$x(t + \Delta t) = 2x(t) - x(t - \Delta t) + \ddot{x}\Delta t^2 \quad (3)$$

where we have dropped all terms of order  $\Delta t^4$  and higher. Note that Eq. 3 does not explicitly contain the particle-velocities. For more details on the integration of the equations of motion of a classical many-body system, the reader is referred to<sup>1</sup>. It should be noted that finite difference schemes such as Eq. 3 cannot be used to solve the equations of motion of 'hard-core' systems. For a review of the numerical techniques that can be used in the latter case, the reader is referred to Ref. 12.

## 4. Choice of Technique

Having introduced both the Monte Carlo and the Molecular Dynamics methods, we must now address the question which technique should be used when. Actually, this question is not as clear-cut as it may seem, because there exist, in fact, a great number of modified MD and MC techniques to compute averages in various ensembles. All these techniques aim to estimate the

equilibrium-average of a particular observable in one ensemble or another. However, in an actual simulation the observable is sampled over a finite time-interval along a trajectory in phase-space (MD), or along a random walk in configuration-space (MC). If a simulation technique is to be useful, the average accumulated in such a sampling procedure should approach the correct ensemble-average, in the limit that the length of the run tends to infinity.

Usually, the equivalence of the MD and MC averages is simply assumed. In the case of Molecular Dynamics, this assumption is equivalent to the 'ergodic hypothesis' of statistical mechanics. For convenience, we shall use the same terminology in the case of Monte Carlo simulations. Non-ergodic behaviour should be distinguished from differences between time and ensemble-averages that may be observed when the computer simulations are too short to sample the accessible phase-space adequately. True non-ergodic behaviour is observed when some parts of the 'permissible' phase-space simply cannot be reached at all, even in an infinitely long simulation. In practice, it is often difficult to distinguish between inadequate sampling due to the limited duration of a simulation and true non-ergodicity, if only because simulations are not infinitely long.

Both Monte Carlo and Molecular Dynamics simulations may suffer from incomplete sampling of the accessible phase-space. The most common example is the simulation of a meta-stable phase, such as for instance an undercooled liquid or a meta-stable crystalline phase. We shall come back to this point in Section 6. There are, however, a number of cases where phase-space is sampled much less efficiently by Molecular Dynamics simulation than by Monte Carlo. This happens, for instance, if the system has certain modes of vibration that are weakly coupled to the remaining degrees of freedom. This is quite a common phenomenon in a low-temperature solid, where long-wavelength phonons may have very long life-times. Another example is a high-frequency internal vibration of a molecule. Energy exchange between such a mode and the other degrees of freedom may be extremely slow in a MD simulation. In contrast, Monte Carlo does not suffer from this particular equilibration problem.

Another situation where the 'unphysical' nature of Monte Carlo moves can be exploited is in (binary) mixtures, in particular when the interdiffusion of the two species is slow. An example is a solid solution. In such solutions the local composition around an atom of species 1 will differ from the overall composition. It is almost impossible to study such changes in local composition using Molecular Dynamics, because particle diffusion in a solid can be a very slow process. In contrast, in a Monte Carlo simulation one may define a trial move which swaps a randomly selected pair of particles of species 1 and 2. If the particles are not too dissimilar, such moves will have a reasonable chance of acceptance, and local compositions can equilibrate rapidly.

However, Monte Carlo is not always the most efficient technique to sample phase-space. There are many cases where the route from one pocket in phase-space to another requires a collective rearrangement of the coordinates of many particles: examples are conformational changes in large molecules and structural phase-transitions in solids. In such cases, Molecular Dynamics often finds a 'natural' reaction-path from one state to the other, where random and uncorrelated Monte Carlo trial moves are much less successful.

#### **4.1. Other Ensembles**

In a conventional MD simulation, the total energy  $E$  and the total linear momentum  $P$  are constants of motion. Hence, MD simulations measure (time-) averages in an ensemble that is very similar to the microcanonical (see Ref. 13), namely the constant-NVE-p ensemble. In contrast, a conventional Monte Carlo simulation probes the canonical (i.e. constant-NVT)

ensemble. The fact that these ensembles are different leads to observable differences in the statistical averages that are computed in MD and MC simulations. Most of these differences disappear in the thermodynamic limit and are already relatively small for systems of a few hundred particles. However, the choice of ensemble does make a difference when computing the mean-square value of *fluctuations* in thermodynamic quantities. Fortunately, techniques exist to relate fluctuations in different ensembles<sup>14</sup>. Moreover, it is nowadays common practice to carry out Molecular Dynamics simulations in ensembles other than the microcanonical. In particular, it is possible to do Molecular Dynamics at constant pressure<sup>15</sup>, at constant stress<sup>3</sup> and at constant temperature<sup>16</sup>. The choice of ensembles for Monte Carlo simulations is even wider: isobaric-isothermal<sup>17,18</sup>, constant-stress-isothermal<sup>5</sup>, Grand-canonical (i.e. constant- $\mu VT$ )<sup>19,20</sup> and even micro-canonical<sup>21</sup>. A recent addition to this list is a Monte Carlo method which employs the 'Gibbs'-ensemble<sup>22</sup>. The latter technique was developed to study phase-coexistence in moderately dense (multi-component) fluids. The 'Gibbs'-method maintains the coexisting phases at equal temperature, pressure and chemical potential.

Clearly, the sheer number of different MC and MD techniques makes it impossible to discuss them in any detail in the present introductory Chapter. However, it is important that the reader be aware that this wide choice of techniques exists. Technical details about most of these simulation methods can be found in Ref.s 1 and 23. I wish to add one cautionary remark: in MD simulations at constant pressure, stress or temperature, additional dynamical variables are introduced that act as manostat/thermostat. The time-evolution of the particle-coordinates in such simulations is governed by equations-of-motion that contain these artificial variables. Although the effect of these extra variables on the particle-dynamics may be small, it is nevertheless advisable to stick to conventional micro-canonical MD if one is primarily interested in the study of dynamical properties. For static equilibrium properties, all of the above methods (MC and MD) should be fine.

#### **4.2. Molecular Dynamics or Monte Carlo ?**

From the discussion in Section 4.1 it is probably clear that the distinction between Molecular Dynamics and Monte Carlo simulations is not all that sharp. Most ensembles of practical importance can be simulated using both techniques. Thus, the choice of one or the other must be dictated by other considerations. All other things being equal, the Molecular Dynamics method is certainly preferable, because it yields information about the dynamical properties of the system under consideration. As was discussed above, MD simulations may sometimes run into 'ergodicity' problems, where MC simulations do not. In such a case it may be preferable to use the Monte Carlo technique, or a hybrid method.

Sometimes the reason to prefer Monte Carlo simulations is much more mundane. It may simply be that, as the expressions for the potential energy function become more complex, the explicit evaluation of the forces and torques for a Molecular Dynamics program becomes quite cumbersome. This implies that there is a distinct risk of introducing errors in the MD code, unless computer-algebra is used to derive the correct expressions. In such cases it is safest to start with a Monte Carlo simulation.

### **5. "Measurements"**

In the previous sections we have described the core of a program to simulate classical many-body systems. In the present section we discuss 'measurements' during such a simulation.

Deciding what quantity to measure during a simulation is a problem, not because such measurements are difficult (in fact, most are quite trivial), but because there is such a wide choice of quantities to measure. Any quantity that can be expressed as an average over phase-space of some function of the particle coordinates and momenta can be measured during a simulation. For instance, in a Monte Carlo simulation, we can measure, apart from the primary thermodynamic variables ( $E, V, T, P, N$ ), the heat-capacity  $C_v$ , the isothermal compressibility  $\chi_T$  and the radial distribution function  $g(r)$  (or, equivalently, the structure factor  $S(k)$ ). Molecular Dynamics simulations offer, in addition, the possibility of measuring transport-properties such as the self-diffusion constant  $D$ , the shear-viscosity  $\eta$  (and the bulk-viscosity  $\zeta$ ), the thermal conductivity  $\lambda_T$  and the dynamical structure-factor  $S(k, \omega)$ . This list is far from exhaustive. Moreover, we are not limited to the computation of quantities that can be measured in real experiments. We can gain insight into the microscopic structure and dynamics of a system by making 'snapshots' of the molecular configurations, or by computing any function of the particle-coordinates and momenta that we consider illuminating. A discussion of computer- 'measurements' is therefore open-ended, and an enumeration is not particularly useful. Rather, I wish to make a few general remarks about the accuracy of measurements in a simulation. The actual examples of computer 'measurements' will follow in the sections that deal with computer simulations of liquid crystals.

### 5.1. Error Estimates

Before discussing error estimates in MC and MD simulations, it is useful to recall what quantities cannot be measured at all in a standard MC or MD simulation. In a simulation one measures averages over phase-space of functions of the particle coordinates and momenta. However, it is not possible to measure directly the *volume* of the accessible phase-space. This volume determines the entropy  $S$  of a system, and thereby the Helmholtz free-energy  $F$  and the chemical potential  $\mu$ . We refer to such quantities as 'thermal', to distinguish them from the 'mechanical' quantities that can be expressed as a function of the phase-space coordinates. Methods to compute thermal quantities are discussed in Section 6. Another situation where MC and MD simulations on a small system cannot be used is in the study of critical phenomena or, for that matter, any situation where correlations over distances much larger than (or incommensurate with) the periodic box play an important role. And finally, *classical* MC and MD will clearly fail if quantum effects become important.

Let us now consider the measurement of a dynamical quantity  $A$  in a Molecular Dynamics simulation (the present discussion applies, with minor modifications, to Monte Carlo simulations). During a simulation of length (that is, duration)  $T$ , we obtain the following estimate for the equilibrium-average of  $A$

$$A_T = (1/T) \int_0^T A(t) dt \quad (4)$$

where the subscript on  $A_T$  refers to averaging over a finite time  $T$ . If the ergodic hypothesis is justified then  $A_T \rightarrow \langle A \rangle$ , as  $T \rightarrow \infty$ , where  $\langle A \rangle$  denotes the ensemble-average of  $A$ .

Let us now estimate the variance in  $A_T$   $\langle (\Delta A_T)^2 \rangle$

$$\begin{aligned} \langle (\Delta A_T)^2 \rangle &= \langle A_T^2 \rangle - \langle A_T \rangle^2 \\ &= (1/T^2) \int_0^T \int_0^T \langle (A(t) - \langle A \rangle)(A(t') - \langle A \rangle) \rangle dt dt' \end{aligned} \quad (5)$$

Note that  $\langle (A(t) - \langle A \rangle)(A(t') - \langle A \rangle) \rangle$  in Eq. 5 is simply the time-correlation function of fluctuations in the variable  $A$ . Let us denote this correlation function by  $C_A(t' - t)$ . If the duration of the sampling  $T$  is much larger than the characteristic decay time  $\tau_A$  of  $C_A$  then we may rewrite Eq. 5 as:

$$\langle (\Delta A_T)^2 \rangle \approx (2/T) \int_0^\infty C_A(t'') dt'' \approx (2\tau_A/T) C_A(0) \quad (6)$$

In the last equation we have used the definition of  $\tau_A$  as the integral from 0 to  $\infty$  of the normalized correlation function  $C_A(t)/C_A(0)$ . The relative variance in  $A_T$  is therefore given by:

$$\frac{\langle (\Delta A_T)^2 \rangle}{\langle A \rangle^2} \approx (2\tau_A/T) \frac{\langle A^2 \rangle - \langle A \rangle^2}{\langle A \rangle^2} \quad (7)$$

Eq. 7 clearly shows that the root-mean-square error in  $A_T$  is inversely proportional to  $(\tau_A/T)^{1/2}$ . This result is hardly surprising. It simply states the wellknown fact the variance in a measured quantity is inversely proportional to the number of uncorrelated measurements. In the present case, this number is clearly proportional to  $T/\tau_A$ . This result may be trivial, but it is nevertheless very important, because it shows directly how the lifetime and amplitude of fluctuations in an observable  $A$  affect the statistical accuracy. This is of particular importance in the study of fluctuations associated with hydrodynamical modes or pretransitional fluctuations near a symmetry-breaking phase transition. Such modes usually have a characteristic life-time that is proportional to the square of their wavelength. This is another reason why it is so difficult to study continuous phase transitions by MD. In order to minimize the effects of the finite system-size on such phase transitions, it is preferable to study systems with a box-size  $L$  that is large compared with all relevant correlation-lengths in the system. However, due to the slow decay of long-wavelength fluctuations, the length of the simulation needed to keep the relative error fixed should be proportional to  $L^2$ . As the CPU time for a run of fixed length is proportional to the number of particles (at best), the CPU-time needed to maintain constant accuracy increases quite rapidly with the linear dimensions of the system (e.g. as  $L^5$  in three dimensions).

There is another aspect of Eq. 7 that is not immediately obvious, namely that it makes a difference whether or not the observable  $A$  can be written as a sum of uncorrelated single-particle properties. If this is the case, then it is easy to see that  $\langle A^2 \rangle - \langle A \rangle^2 / \langle A \rangle^2$  is inversely proportional to the number of particles,  $N$ . To see this, consider the expressions for  $\langle A \rangle$  and  $\langle A^2 \rangle - \langle A \rangle^2$  in this case:

$$\langle A \rangle = \sum_{i=1}^N \langle a_i \rangle = N \langle a \rangle \quad (8)$$

and

$$\langle A^2 \rangle - \langle A \rangle^2 = \sum_{i=1}^N \sum_{j=1}^N \langle a_i - \langle a \rangle \rangle \langle a_j - \langle a \rangle \rangle \quad (9)$$

If the fluctuations in  $a_i$  and  $a_j$  are uncorrelated, then we find:

$$\frac{\langle A^2 \rangle - \langle A \rangle^2}{\langle A \rangle^2} = (1/N) \frac{\langle a^2 \rangle - \langle a \rangle^2}{\langle a \rangle^2} \quad (10)$$

From Eq. 10 it is clear that the statistical error in a single-particle property is inversely proportional to  $\sqrt{N}$ . Hence, for single-particle properties the accuracy improves as one goes to larger systems (for fixed length of the simulation). In contrast, no such advantage is to be gained when computing truly collective properties. This is one more reason why bigger is not always better. A more detailed discussion of statistical errors in collective and single-particle time-correlation functions can be found in Ref.s 24 and 25. Systematic techniques to measure statistical errors in a simulation are discussed in Ref.s 1 and 26.

## 6. Phase Transitions

As was mentioned in Section 5.1, 'thermal' quantities such as the free energy  $F$ , the entropy  $S$  and the chemical potential  $\mu$  cannot be measured directly in a computer simulation because they depend explicitly on the accessible volume in phase-space. However, knowledge of such thermal quantities (in particular  $\mu$ ) is usually necessary to locate the coexistence line for a first-order phase-transition. At first sight this knowledge may appear superfluous. After all, a computer simulation mimics the behaviour of a real solid or liquid. If the simulation is ergodic it should spontaneously transform to whatever phase is thermodynamically most stable, and then we would know all there is to know. Unfortunately, this approach does not work, at least not for strong first-order phase transitions such as freezing. At a solid-solid or solid-liquid phase transition very strong hysteresis effects are usually observed in a simulation. In fact, it is very difficult to nucleate a crystal from a liquid during a simulation. Hence, to locate the point where two phases coexist, we must compute the chemical potential of the homogeneous phases at the same temperature and pressure and find the point where the two  $\mu$ 's are equal. General methods to compute  $\mu$  and related thermal quantities by computer simulation are discussed in Ref. 27. Here I wish to focus exclusively on those techniques that should work for dense systems. In these techniques it is usually the free energy  $F$  rather than the chemical potential  $\mu$  that is computed.

When discussing techniques to measure free energies, it is useful to recall how such quantities are measured in real experiments. In the real world free energies cannot be obtained from a single measurement either. What can be measured, however, is the derivative of the free energy with respect to volume  $V$  and temperature  $T$ :

$$\left(\frac{\partial F}{\partial V}\right)_{NT} = -P \quad (11)$$

and

$$\left(\frac{\partial F}{\partial T}\right)_{NV} = -E \quad (12)$$

Here  $P$  is the pressure and  $E$  the energy of the system under consideration. The trick is know to find a reversible path that links the state under consideration to a state of known free energy. The change in  $F$  along that path can then simply be evaluated by integration of Eq.s 11 and 12.

In the real world the free energy of a substance can only be evaluated directly for a very limited number of thermodynamic states. One such state is the ideal gas phase, and another is the perfectly ordered ground state at  $T = 0$  K. In computer simulations, the situation is quite similar. In order to compute the free energy of a dense liquid, one may construct a reversible

path to the very dilute gas phase. It is not really necessary to go all the way to the ideal gas. However, at least one should reach a state that is sufficiently dilute that the free energy can be computed accurately, from knowledge of the first few terms in the virial expansion of the compressibility factor  $PV/Nk_B T$ , or that the chemical potential can be computed by other means (see Ref. 27).

For solids, the ideal gas reference state is less useful (although techniques have been developed to construct a reversible path from a dense solid to a dilute (lattice-) gas<sup>28</sup>). The obvious reference state for solids is the harmonic lattice. Computing the absolute free energy of a harmonic solid is relatively straightforward, at least for atomic and simple molecular solids. However, not all solid phases can be reached by a reversible route from a harmonic reference state. For instance, in molecular systems it is quite common to find a strongly anharmonic plastic phase just below the melting line. This plastic phase is not (meta-) stable at low temperatures.

Fortunately, in computer simulations we do not have to rely on the presence of a 'natural' reversible path between the phase under study and a reference state of known free energy. If such a path does not exist, we can construct an artificial path. This is in fact a standard trick in statistical mechanics (see e.g. Ref. 29). It works as follows: Consider a case where we need to know the free energy  $F(V,T)$  of a system with a potential energy function  $U_1$ , where  $U_1$  is such that no 'natural' reversible path exists to a state of known free energy. Suppose now that we can find another model system with a potential energy function  $U_0$  for which the free energy *can* be computed exactly. Now let us define a generalized potential energy function  $U(\lambda)$ , such that  $U(\lambda=0) = U_0$  and  $U(\lambda = 1) = U_1$ . The free energy of a system with this generalized potential is denoted by  $F(\lambda)$ . Although  $F(\lambda)$  itself cannot be measured directly in a simulation, we can measure its derivative with respect to  $\lambda$ :

$$\left( \frac{\partial F}{\partial \lambda} \right)_{NVT\lambda} = \left\langle \frac{\partial U(\lambda)}{\partial \lambda} \right\rangle_{NVT\lambda} \quad (13)$$

If the path from  $\lambda = 0$  to  $\lambda = 1$  is reversible, we can use Eq. 13 to compute the desired  $F(V,T)$ . We simply measure  $\langle \partial U / \partial \lambda \rangle$  for a number of values of  $\lambda$  between 0 and 1. Typically, 10 quadrature points will be sufficient to get the absolute free energy per particle accurate to within 0.01  $k_B T$ . It is, however, important to select a reasonable reference system. One of the safest approaches is to choose as a reference system an Einstein crystal with the same structure as the phase under study. This choice of reference system makes it extremely improbable that the path connecting  $\lambda = 0$  and  $\lambda = 1$  will cross an (irreversible) first order phase transition from the initial structure to another, only to go back to its original structure for still larger values of  $\lambda$ . Nevertheless, it is important that the parametrization of  $U(\lambda)$  be chosen carefully. Usually, a linear parametrization (i.e.  $U(\lambda) = \lambda U_1 + (1-\lambda)U_0$ ) is quite satisfactory. But occasionally such a parametrization may lead to weak (and relatively harmless) singularities in Eq. 13 for  $\lambda \rightarrow 0$ . More details about such free energy computations can be found in Ref.s 27, 30.

Before proceeding to the actual simulations of liquid crystals, I wish to point out that it is often not trivial to construct a reversible path that will link a liquid crystalline phase to a state of known free energy. Usually, the liquid-crystalline phase of interest will be separated by first order phase transitions from both the dilute gas and the low temperature (harmonic) solid. In the case of the nematic phase this problem has been resolved by switching on a strong ordering field. In the presence of such a field, the first-order isotropic-nematic transition is suppressed and a reversible expansion to the dilute gas becomes possible<sup>31</sup>. For the calculation of free energies of smectic and columnar phases, other techniques have to be used. Although I do not wish to go

into any detail here, I wish to point out two fairly general approaches: the first is based on the fact that a smectic phase can be considered as a 1 dimensional solid stacking of 2D fluid layers, while a columnar phase resembles a 2D crystal of 1D fluid columns. In Ref. 30, a technique is described that makes it possible to reversibly decompose such smectic (columnar) phases into isolated fluid layers (columns). However, this approach has, to my knowledge, not yet been applied to such liquid crystals.

It should be stressed that such absolute free energy calculations need not be repeated for every model that we may care to study. For instance, if we have computed the absolute free energy of one state point in the smectic phase of rod-like molecules with an aspect ratio of 5 (say), then we can compute the free energy of the smectic phase of similar molecules with another aspect ratio simply by computing the reversible work needed to change the shape of our model particles from the initial aspect ratio to the desired value. An example of such a technique, in a slightly different context, can be found in Ref. 32.

### 6.1. Isotropic-nematic Transition

With computer simulation it is, in principle, possible to compute the properties of any model for a classical many-body system. The choice of the model is determined by the nature of the question that we wish to answer. In the present case we are interested in crystalline and liquid-crystalline ordering in simple models for molecular liquids.

What is the most appropriate model? There is no unique answer to this question. Several mechanisms have been invoked to explain the onset of liquid crystalline ordering (see e.g. Ref. 33). Onsager<sup>34</sup> showed that nons-spherical excluded-volume effects are all that is needed to induce an isotropic to nematic transition in a system of thin, rigid rods. However, the Maier-Saupe mean-field theory shows that the same transition may also be caused by anisotropic attraction forces<sup>35</sup>. In addition, there are other more factors that can play a role. For instance, for thermotropics, the tendency of molecules to form liquid crystals depends strongly on the nature of the flexible side-chains attached to the rigid core of the molecule<sup>36</sup>, while the angle-dependence of the effective attractive forces depends on the shape of the non-spherical hard core of the molecule<sup>37</sup>. For lyotropics, molecular flexibility and polydispersity both have a pronounced effect on the tendency to form a liquid crystal. All these factors are real. However, it would be very unwise to try to take everything into account at once. It is inevitable that a choice must be made between primary and secondary factors.

In the case of freezing of molecular liquids the situation is similar: attraction, repulsion and flexibility all play a role. For instance, we know that the presence of flexible side-chains in a molecule makes the formation of a molecular crystal entropically less favourable. Only for atomic liquids is the picture clear. Since the work of Alder and Wainwright<sup>38</sup> it has been known that the freezing of atomic liquids is primarily an excluded volume effect. That does not imply that attractive forces do not affect the location of the freezing point (they do). But the structure of the coexisting phases is largely determined by the harsh repulsive interactions between the atoms. The effect of attraction can be considered a perturbation<sup>39</sup>.

If freezing can be understood in terms of excluded volume effects alone, it is natural to ask how far we can push this idea in the case of liquid crystalline ordering. Our aim then is to study the simplest possible hard-core models that may form both crystalline and liquid-crystalline phases.

It should be noted that an alternative approach has been followed by Luckhurst and collaborators<sup>40</sup>. Following the pioneering work of Lebwohl and Lasher<sup>41</sup>, these authors focused

on the effect of anisotropic intermolecular interactions of the form  $v_{ij} = -J_{ij}P_2(\cos\theta_{ij})$ . The choice of the Lebwohl-Lasher model was inspired by the original justification of the Maier-Saupe theory in terms of anisotropic dispersion forces. It should be noted that in simulations of models such as the one introduced by Lebwohl and Lasher it is assumed that the molecules reside on a periodic lattice. In that case the 'I-N' transition may also be interpreted as a rotational order-disorder transition in a crystalline solid.

Computer simulations of hard-core models for two-dimensional liquid crystals were pioneered by Vieillard-Baron in the early seventies<sup>42</sup>. Vieillard-Baron also made much progress towards the study of three-dimensional model systems<sup>43</sup>, but did not observe spontaneous nematic ordering in 3D. The first systematic simulation study of a three-dimensional hard-core nematogen was performed by Frenkel and Mulder<sup>31</sup> who studied a system of hard ellipsoids-of-revolution for a range of length-to-width ratios.

The shape of hard ellipsoids of revolution is characterized by a single parameter,  $x$ , the ratio of the length of the major axis ( $2a$ ) to that of the minor axis ( $2b$ ):  $x = a/b$ . Prior to the simulations reported in Ref. 31, the phase behaviour of hard spheroids<sup>29</sup> was only known for a few special values of  $x$ , viz:

- (1)  $x = 1$  : hard spheres, which freeze at  $2/3$  of close packing<sup>44</sup>;
- (2)  $x \rightarrow \infty$  : thin hard needles, because this limit is equivalent to the Onsager model; this latter system has a transition to the nematic phase at vanishing volume fraction;
- (3)  $x \rightarrow 0$  : thin hard platelets, which also form a low-density nematic<sup>45</sup>.

The simulations of Ref. 31 were performed for values of  $x$  between 3 and  $1/3$ . In order to locate all phase transitions, the absolute free energy of every phase was computed. Fig. 1 shows how the stability of the different phases of hard ellipsoids depends on their length-to-width ratio.

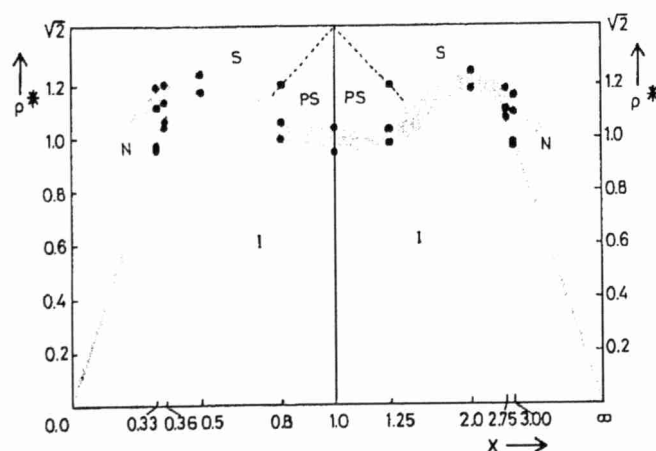


Fig. 1. 'Phase diagram' of a system of hard ellipsoids of revolution<sup>31</sup>. The ratio of the length of the semi-major to the semi-minor axis is denoted by  $x$ . The reduced density  $p^*$  is defined such that the density of regular close packing is equal to  $\sqrt{2}$  for all  $x$ . The shaded areas indicate two-phase regions associated with a first-order phase transition. The following phases can be distinguished: I: Isotropic fluid, S: Orientationally ordered crystalline solid, PS: Orientationally disordered ('plastic') crystal, and N: Nematic liquid-crystalline phase. The densities of coexisting phases at a first order phase transition (black dots) were computed in a free-energy calculation. Note that no stable nematic is possible for  $0.4 < x < 2.5$ .

Four distinct phases can be identified, namely the low-density isotropic fluid, an intermediate-density nematic liquid crystalline phase, which is only stable if the length-to-width ratio of the ellipsoids is larger than 2.5 or less than 0.4, and a high-density orientationally ordered solid phase. In the case of weakly anisometric ellipsoids, an orientationally disordered solid phase was also observed. One thing to note about the phase transitions in the hard-ellipsoid system is that for particles with  $3 \geq x \geq (1/3)$  the relative density-jump at the I-N transition is much smaller than for the Onsager model. Typically, the density changes only by some 2% at the I-N transition, hence the very large density discontinuity at the I-N transition in the Onsager model (more than 20%) is peculiar to long rods and not to hard-core models in general.

Perhaps the most striking feature of the phase diagram in Fig. 1 is the near symmetry between the behavior of oblate and prolate ellipsoids with inverse length-to-width ratios. Prolate-oblate ( $x \rightarrow 1/x$ ) symmetry of ellipsoids is to be expected at *low* densities because the second virial coefficient  $B_2(x)$  equals  $B_2(1/x)$ . However, no such relation holds between the third and higher virial coefficients. To give a specific example: in the limit  $x \rightarrow \infty$  (the Onsager limit),  $B_3/B_2^2$ , whereas for  $x \rightarrow 0$  (hard platelets<sup>45</sup>)  $B_3/B_2^2 \rightarrow 0.4447(3)$ . Hence there is no reason to expect any exact symmetry in the phase diagram of hard ellipsoids of revolution. For larger anisotropies than studied in the simulations of Ref. 31 one should expect to see asymmetric behaviour in the location of the isotropic-nematic transition. In fact, Allen has performed<sup>46</sup> simulations of ellipsoids with aspect ratios 5,10,0.2 and 0.1. These simulations show that, as the molecular anisotropy increases, the Isotropic-Nematic transition continues to shift to lower densities. This is to be expected in view of the known limiting behavior of infinitely thin hard platelets and infinitely thin hard rods (see above). However, in Ref. 46 the exact location of the isotropic-nematic transition is not computed.

Even though we expect to see appreciable prolateoblate asymmetry in the location of the isotropic-nematic transition for highly anisometric spheroids, it is doubtful if the near symmetry

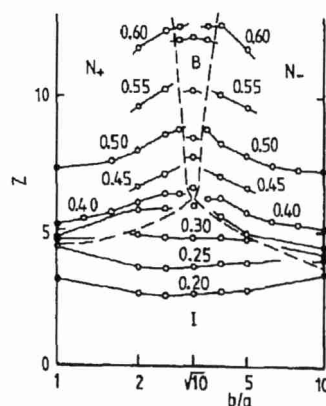


Fig.2.  $Z = PV/Nk_B T - 1$  of a system of biaxial ellipsoids with axial ratio  $c/a = 10$  while  $b/a$  varies between 1 (prolate limit) and 10 (oblate limit)<sup>46</sup>. In this figure  $b/a$  is represented on a logarithmic scale. The dashed curves separate state points belonging to the different phases:  $I$  denotes the isotropic phase,  $N+$  the 'rod-like' nematic phase,  $N-$  the 'plate-like' nematic phase and  $B$  the biaxial phase. The drawn curves connect the measured state-point data within one phase at a given reduced density  $\rho/\rho_{\text{close-packed}}$ . Note that the biaxial phase ends in a tri-critical point at an aspect ratio  $a/b = \sqrt{10}$ . This behavior is in agreement with the theoretical predictions of Mulder<sup>49</sup>. This figure was reproduced with permission of Dr. Allen.

of the melting line will be much affected. Strongly aligned rods and platelets follow the same equation of state ( $P = 3p$ ) and a simple estimate of the melting point of very anisometric ellipsoids<sup>47</sup> suggests that in the limit  $x \rightarrow \infty$  the symmetry between oblate and prolate ellipsoids is still present.

More recently, Allen has studied the effect of molecular biaxiality on the mesogenic properties of hard ellipsoids<sup>48</sup>. In particular, Allen studied the nature of the liquid-crystalline phase as a prolate spheroid was made increasingly biaxial and was finally transformed into an oblate spheroid. In this case it was found that the rod-like and plate-like nematic phases are separated by a biaxial phase. Fig. 2 shows how the stability of the different liquid-crystalline phases depends on the molecular biaxiality.

### 6.2. Theoretical Description

The numerical simulation of the phase diagram of hard ellipsoids of revolution provided theoreticians with an opportunity to compare analytical theories for the isotropic-nematic transition with 'exact' numerical data. Several rather different theoretical approaches have been tested in this way. Actually, this work was predated by the scaled-particle for the isotropic-nematic transition constructed by Cotter and Martire<sup>50,51</sup>. However, this scaled-particle theory was worked out for hard spherocylinders and could only be compared with simulation data for the isotropic phase.

The first statistical mechanical theory for the I-N transition in a fluid of hard ellipsoids was developed by Mulder<sup>53</sup>, who followed the so-called 'y-expansion' approach of Barbooy and Gelbart<sup>52</sup>. Mulder found that the y-expansion led to a slight over-estimate of the pressure in the isotropic phase and that the isotropic-nematic transition was predicted to occur at too low a density. Moreover, the density-jump at this transition was predicted to be larger than observed in the simulations. However, the very symmetric appearance of the phase-diagram was well reproduced by the theory of Ref. 53.

Subsequently, several authors have applied density-functional theory to the study of the isotropic-nematic transition of hard ellipsoids. The first such theory was formulated by Singh and Singh<sup>54</sup>. These authors also discussed the freezing transition of hard ellipsoids and used density-functional theory to estimate the stability of the plastic crystalline state. Subsequently, alternative density-functional theories for hard ellipsoids of revolution were presented by Baus et al.<sup>55</sup> and by Marko<sup>56</sup>. A good discussion of the relative merits of these theories can be found in the article by Colot, Wu, Xu and Baus<sup>57</sup>.

A rather different approach was followed by Perera et al.<sup>58</sup>. These authors studied the generalization to convex hardbody fluids of the Percus-Yevick (PY) and Hypernetted Chain (HNC) integral equations that are known to be quite successful for simple fluids<sup>29</sup>. Perera et al. found that for hard ellipsoids of revolution the PY approach failed to predict the existence of a stable nematic phase. In contrast, the HNC theory yielded a fair estimate of the location of the isotropic-nematic transition (or, to be more precise, of the density where the isotropic phase becomes mechanically unstable).

### 6.3. Two-dimensional Nematics

Two-dimensional liquid crystals are very different from their 3D counterparts. This can be clearly demonstrated by considering the isotropic-nematic transition in two dimensions. On basis of the Landau theory of phase transitions, we expect that the isotropic nematic transition in two dimensions should be of second order. Density-functional theory<sup>63</sup> predicts the same.

However, the actual situation is much more subtle than that. The point is that two-dimensional nematics are very similar to the two-dimensional Heisenberg system ('2D-xy model') and hence there is a possibility that topological defects have a pronounced effect on the nature of the phase transitions<sup>59</sup>.

In order to see this, let us consider the expression of the Frank free-energy density of a 2D-nematic. We choose the average director along the y-axis. We denote the angle between the average director and the instantaneous local director by  $\theta$ . By analogy to the three-dimensional case<sup>33</sup>, the expression for the deformation free energy is of the form:

$$F_D = \frac{1}{2}K_1(\partial_x n_x)^2 + \frac{1}{2}K_3(\partial_y n_x)^2 = \frac{1}{2}K_1(\partial_x \theta)^2 + \frac{1}{2}K_3(\partial_y \theta)^2 \quad (14)$$

where we have assumed that  $\theta$  is small. We shall simply postulate that the deformation free energy of a 2D nematic is given by Eq. 14. Moreover, we shall assume for the sake of convenience that  $K_1 = K_3$ . In that case we obtain a very simple expression for the deformation free-energy density:

$$F_D = \frac{1}{2}K(\nabla\theta)^2 \quad (15)$$

Using this expression, it is easy to compute the elastic contribution to the free energy of a single  $\pi$ -disclination in a 2D-nematic. Consider a circular path (circumference  $2\pi r$ ) around the dislocation core. Along this path, the director rotates over an angle  $\pi$ . Hence  $(\nabla\theta)^2 = (1/2r)^2$ . If we insert this expression in Eq. 15 and integrate from the dislocation core (radius  $a_0$ , say) to  $L$  (the linear dimension of the system) then we find that the elastic energy of an isolated disclination is:

$$F_{el} = \frac{1}{2}K \int_{a_0}^L \frac{2\pi r}{4r^2} dr = \frac{\pi K}{4} \log(L/a_0) \quad (16)$$

Clearly,  $F_{el} \rightarrow \infty$  if  $L \rightarrow \infty$ .

This would seem to suggest that no free disclinations are possible in a 2D nematic. However, we should also consider the 'configurational entropy' of a single disclination, i.e. the entropy  $k\log\Omega$  associated with the number of distinct ways in which we can place a dislocation in a two-dimensional area  $L^2$ . If we use  $a_0$  as our unit of length, then the configurational entropy is given by  $k\log(L/a_0)^2$  (where we have neglected an additional constant, independent of system size). Combining this expression for the configurational entropy with our expression for the elastic free energy (Eq. 16) we obtain the following expression for the total free energy of a single disclination in a 2D nematic:

$$F_{total} = \left( \frac{\pi K}{4} - 2kT \right) \log(L/a_0) \quad (17)$$

Eq. 17 suggests that if  $kT < (\pi K/8)$  no free disclinations are possible, whereas for  $kT > (\pi K/8)$  spontaneous generation of free disclinations may take place. However, if a nematic contains a finite concentration of free disclinations, orientational correlations are destroyed over distances longer than the characteristic separation of the free defects and the resulting phase is

an isotropic fluid. This simple version of the Kosterlitz-Thouless scenario for defect mediated phase transitions predicts that the nematic phase cannot be stable above a critical temperature  $kT^* = (\pi K/8)$ . At that temperature there is a continuous phase transition (of 'infinite' order) from the nematic to the isotropic phase. However, there is an alternative possibility: namely that the I-N transition is simply first order. But if the I-N transition is of first order then this transition must occur *before* the nematic phase has reached the point where it becomes unstable with respect to the formation of free disclinations: i.e. at a first-order I-N transition the following inequality must hold:

$$K > \frac{8kT}{\pi}$$

This condition also follows from the more rigorous version of the KT-theory.

Note that our discussion of the disclination-mediated I-N transition was based on the assumed form of the Frank free energy (Eq. 14). It should be stressed that this form of the deformation free energy has quite drastic consequences for the nature of orientational order in 2D nematics. In particular, it implies that there exist no true long-ranged orientational order in such systems. We define the  $l$ -th orientational correlation function as:

$$g_l(r) \equiv \langle \cos 2l(\theta(0) - \theta(r)) \rangle = Re \langle \exp[-2il(\theta(0) - \theta(r))] \rangle \quad (18)$$

Using the fact that the free energy (Eq. 15) is quadratic in  $\theta(k)$ , it is easy to show that  $g_l(r)$  has the following form:

$$g_l(r) = \left( \frac{r}{a_0} \right)^{-\frac{2l^2 kT}{\pi K}} \equiv \left( \frac{r}{a_0} \right)^{-\eta_l} \quad (19)$$

where the last term on the right-hand side of Eq. 19 defines the exponent  $\eta_l$ . Note that this equation implies that, provided that Eq. 14 is valid, there is no true long-range orientational order in a 2D nematic, but algebraic or 'quasi long-range' order. Similarly, it can be shown that the order parameter  $\langle \cos 2\theta \rangle$  also vanishes algebraically with increasing system size:

$$\langle \cos 2\theta \rangle \propto \left( \frac{L}{a_0} \right)^{-\frac{kT}{\pi K}} \quad (20)$$

Now recall that a 2D nematic is only expected to be stable against the spontaneous generation of free disclinations, when  $K$  is larger than  $\pi/(8kT)$ . Hence, at the  $K$ - $T$  transition the orientational correlation functions and the nematic order parameter must satisfy the following relations:

$$g_l(r) = \left( \frac{r}{a_0} \right)^{-\frac{l^2}{4}} \quad (21)$$

$$\langle \cos 2\theta \rangle \propto \left( \frac{L}{a_0} \right)^{-\frac{1}{4}} \quad (22)$$

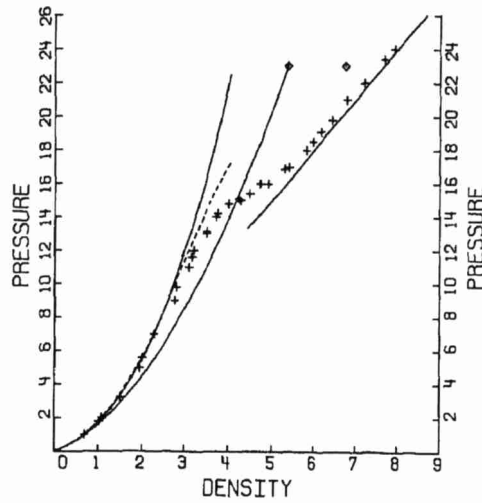


Fig.3. Equation of state of two-dimensional fluid of infinitely thin hard needles of length 1, as obtained by Monte Carlo simulation<sup>61</sup>. Note that in this figure the reduced pressure is the independent variable. The reduced density  $\rho L^2$  is indicated by crosses, the chemical potential  $\mu$  by triangles. The curves at low pressure were computed using a 5-term virial series. For more details, see Ref. 61.

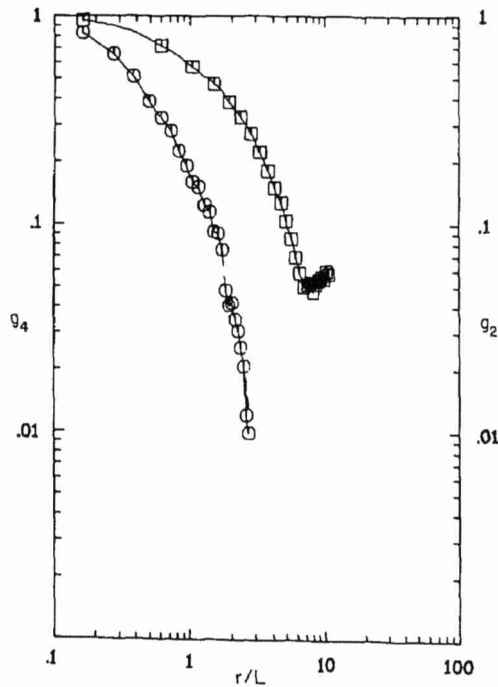


Fig.4. Orientational correlation functions  $g_2 \equiv \langle \cos 2(\phi(0) - \phi(r)) \rangle$  and  $g_4 \equiv \langle \cos 4(\phi(0) - \phi(r)) \rangle$  for a two dimensional system of hard needles of length  $L = 1$ . This figure shows that at a reduced density  $\rho L^2 = 6.75$  the orientational order decays exponentially. In other words, the phase is isotropic.

Two points should be stressed:

- [1] If the I-N transition is first order then, at the transition the exponents of  $g_l$  and  $\langle \cos 2\theta \rangle$  must be less than the critical values given by Eq. 21; and,
- [2] The above arguments rest on the assumption that the deformation free energy is of the form given by Eq. 15.

If this expression is valid, 2D nematics can only have algebraic orientational order. However, it has thus far only been possible to prove the absence of true long-range orientational order for a certain class of short ranged potentials called *separable*<sup>60</sup>. A pair-potential is called separable if the interaction energy of two molecules at fixed center-of-mass separation  $r_{ij}$  depends only on the relative orientation of the two molecular axes  $u_i \cdot u_j$ , but not on  $r_{ij} \cdot u_i$  or  $r_{ij} \cdot u_j$ . Realistic pair-potentials are hardly ever separable.

There are therefore two obvious questions that one could ask about 2D nematics:

- [1] If the pair potential is non-separable, do we find algebraic or true long-range order? and,
- [2] If we find algebraic order, do we observe a first order I-N transition or a continuous one of the Kosterlitz-Thouless type?

To start with the first question: a good starting point would be to choose a pair-potential that is as non-separable as possible. An obvious candidate is a two-dimensional model of infinitely thin hard needles<sup>61</sup>. This pair potential is very non-separable in the sense that, at fixed  $|r_{ij}|$  and fixed  $u_i \cdot u_j$  the pair potential is *not* constant, but may vary between 0 and  $\infty$ . The equation of state of this system is shown in Fig. 3. According to the bifurcation analysis of the corresponding Onsager limit<sup>62</sup> a second-order isotropic-nematic transition is expected at a density  $\rho L^2 = (3\pi/2) = 4.712\dots$  and a pressure  $PL^2 = 11.78\dots$ . At first sight this seems to be quite a reasonable estimate of the I-N transition, because very close to this point the equation of state appears to exhibit a change of slope. However, analysis of the long-range behaviour of the orientational correlation functions and of the system-size dependence of the order-parameter  $\langle \cos 2\theta \rangle$  indicate that the higher density phase is not a stable nematic. The orientational correlation functions decay either exponentially (see Fig. 4) or with an apparent algebraic exponent that is larger than the critical value given in Eq. 21. Only at a density that is almost twice the Onsager transition point does the observed behaviour conform to what is expected for a stable nematic with algebraic order (see Fig. 5). However, at this density the equation of state is completely featureless. Such behaviour is to be expected if the I-N transition is in fact of the *K-T* type.

Subsequently, Cuesta and Frenkel<sup>64</sup> have studied the isotropic to nematic transition in a system of 2D ellipses with aspect ratios 2, 4 and 6. It is found that in all cases where a stable nematic phase is found (aspect ratios 4 and 6), this phase exhibits algebraic orientational order. However, whereas the I-N transition appears to be of the *K-T* type for aspect ratio 6 (and larger), the transition is found to be first order for aspect ratio 4. This implies that in the latter case the 2D nematic undergoes a first-order transition *before* it has reached the point where it becomes absolutely unstable with respect to declination unbinding.

A very puzzling feature is the nature of the high-density phase of 2D ellipses. A snapshot of such a phase is shown in Fig. 6. This phase does not appear to have true crystalline order, nor for that matter, smectic order, yet it does clearly have a large amount of local order. The precise nature of this high density phase is currently under investigation.

I am not aware of any 2D hard-core systems that show anything but quasi-long range nematic order, and I would be very surprised to see true long range orientational order in a 2D liquid crystal in the absence of some kind of positional order. For a discussion of nematic ordering in systems with continuous intermolecular interactions, see Ref. 65.

## 7. Beyond Nematics

The existence of a nematic phase in a system of hard-core molecules is not surprising. In fact, the earliest analysis of any statistical-mechanical model for a liquid-crystalline phase, i.e. Onsager's study of a system of thin hard rods, shows that this simple hard-core system *must* form a nematic phase at sufficiently high density. It would of course be nice if there existed something like the Onsager model for smectics: an exactly solvable model system that exhibits a transition to the smectic A phase. Unfortunately, no such model is known.

Hence, the only way to test approximate 'molecular' theories of the smectic phase is to compare with computer simulations. In the spirit of the Section 6.1 we look for the simplest possible model that will form a smectic phase. In the case of nematics, convex hard-core models are the natural candidates because these constitute the natural generalization of the Onsager model. However, for smectics it is not obvious that hard-core models will work. In fact, in existing textbooks on liquid-crystal physics the possibility of a hard-core smectic is not even discussed. To my knowledge the only pre-simulation article discussing the possibility of hard-core smectics is a paper by Hosino et al.<sup>66</sup> The 'traditional' approach was to ascribe the smectic ordering to

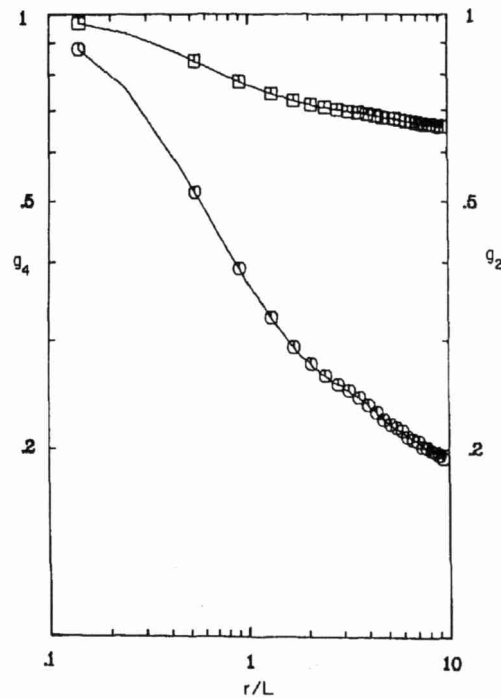


Fig.5. Orientational correlation functions  $g_2 = \langle \cos 2(\phi(0) - \phi(r)) \rangle$  and  $g_4 = \langle \cos 4(\phi(0) - \phi(r)) \rangle$  for a two-dimensional system of hard needles of length  $L = 1$ . This figure shows that at a reduced density  $\rho L^2 = 8.75$  the orientational order decays algebraically. From the values of the algebraic exponents  $\eta_2$  and  $\eta_4$  the effective Frank elastic constant can be computed. At  $\rho = 8.75$  this Frank constant is large enough to make the 2D nematic stable with respect to disclination unbinding. The isotropic-nematic transition is estimated to occur somewhere around  $\rho = 7.5$ . Note that if we had only used Fig. 3 to locate the isotropic-nematic transition! we might have concluded that this transition occurs at a density of approximately 5.0 in reduced units.

attractive interactions between the molecular cores or, alternatively, to the change in packing entropy of the flexible tails of the mesogenic units<sup>36</sup>.

### 7.1. Parallel Molecules

Whereas essentially *any* fluid of sufficiently non-spherical convex hard bodies will form a nematic phase, non-sphericity alone is not enough to form a smectic phase. This is best demonstrated by the following simple example. We know from experiment that in many smectic phases the orientational order parameter  $S \approx 1$ . Let us therefore first consider the possibility of forming a smectic phase in a fluid of *perfectly aligned* molecules ( $S=1$ ). We know that sufficiently nonspherical hard ellipsoids can form a nematic phase (see Section 6.1). It is natural to ask whether a perfectly aligned nematic of hard ellipsoids can transform into a smectic phase. The answer to this question is: *no*. The reason is quite simple. Consider a fluid of ellipsoids with length-to-width ratio  $a/b$  all aligned along the  $z$ -axis (say). Now we perform an affine transformation that transforms all  $z$  coordinates into coordinates  $z'$ , such that  $z' = (b/a)z$ . At the same time we transform to new momenta in the  $z$ -direction:  $p'_z = (a/b)p_z$ . Clearly, this transformation does not change the partition function of the system, and hence all thermodynamic properties of the system are unchanged. However, the effect of this affine transformation is to

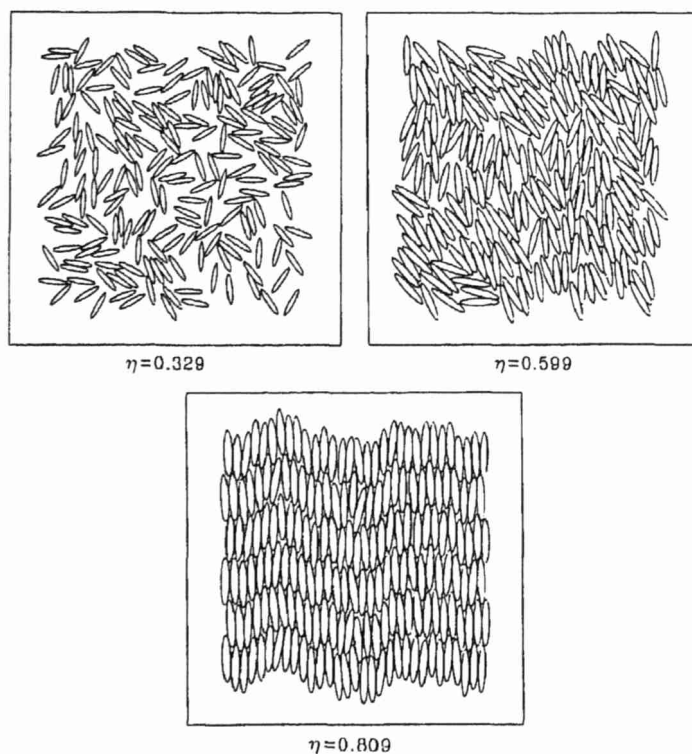


Fig.6. Snapshots of typical configurations of a system of hard ellipses in the isotropic phase ( $\eta = 0.329$ ), near the estimated isotropic-nematic transition ( $\eta = 0.599$ ) and in the high-density phase ( $\eta = 0.809$ ). Although the latter phase exhibits local solid-like ordering, it is not a true (two-dimensional) solid.

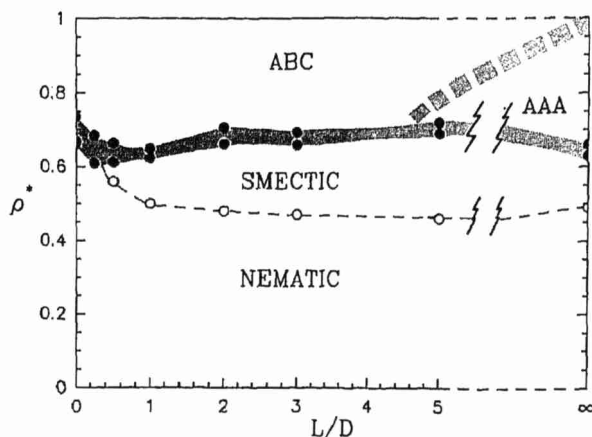


Fig. 7. Schematic 'phase diagram' of a system of parallel hard spherocylinders as obtained by computer simulation<sup>71</sup>. The abscissa indicates the length-to-width ratio  $L/D$ . The ordinate measures the density referred to the density at regular close packing. The dashed area indicates the two-phase region at the first-order freezing transition. For  $L/D < 5$ , the solid consists of 'ABC'-stacked triangular planes. For larger values of  $L/D$ , we find evidence for a hexagonal ('AAA') stacking of the molecules (i.e. triangular lattices stacked on top of one another). At very high densities and large  $L/D$  values we find a pocket where the system appears to form a columnar phase. However, the range of stability of this phase is strongly dependent on the size of the system studied. Although we still observed this columnar phase for a system of 1080 particles, it is conceivable that this phase will disappear altogether in the thermodynamic limit. The dashed curve indicates the nematic-smectic transition.

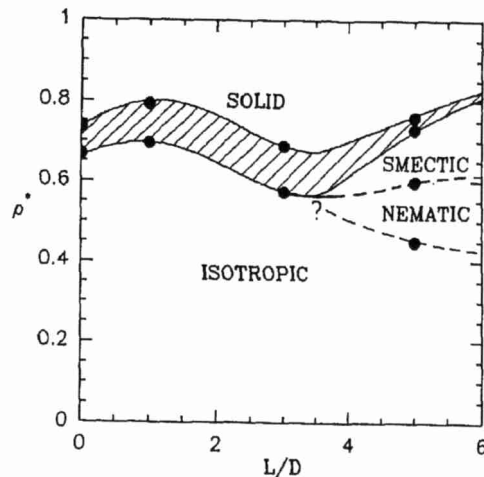


Fig. 8. Phase diagram of a system of freely rotating spherocylinders as a function of the ratio between the length of the cylindrical part ( $L$ ) and the diameter ( $D$ ). The ordinate  $\rho^*$  measures the density divided by the density at regular close packing. The grey (dashed) area is the two-phase region separating the densities of the coexisting solid and fluid phases. The black dots indicate computed phase-coexistence points. The nematic-smectic transition is indicated by a dashed curve, as is the isotropic-nematic transition. Although the latter transition is expected to be of first order, the resolution of the present simulation was insufficient to determine the density discontinuity at this transition. The location of the isotropic-nematic-smectic triple point can only be estimated approximately and is indicated in the figure by a question mark.

change a fluid of parallel ellipsoids into a system of hard spheres. But, as far as we know, hard spheres can only exist in two phases: fluid and crystal. Hence parallel ellipsoids can only occur in the (nematic) fluid phase and in the crystalline solid phase. In particular: no smectic phase is possible. This makes it extremely improbable that a fluid of non-parallel ellipsoids will form a stable smectic. Such a phase is only expected in the unlikely case that the orientational fluctuations would stabilize smectic order<sup>67</sup>.

This example demonstrates that we should be careful in selecting possible models for a hard-core smectics. Surprisingly (and luckily) it has turned out that another very simple hard-core model system, namely a system of parallel hard spherocylinders, does form a smectic phase<sup>69,70</sup>. A stable smectic phase is possible for length-to-width ratios  $L/D \geq 0.5$ . In addition, we find that another phase appears at high densities and larger  $L/D$  values. In small systems, the phase appears to be columnar<sup>70</sup>, but in larger systems the range of stability of the columnar phase shrinks (see Fig. 7) and is largely replaced by a hexagonal solid phase. In order to tell whether the latter phase is indeed truly solid or, for example, smectic-B, would require simulations on systems that contain many more particles than the 1000-2000 that we have thus far been able to study systematically.

At first sight it seems surprising that pure excluded volume effects can give rise to smectic ordering. However, stimulated by the computer-simulation results a number of authors have reexamined<sup>72,73,74,75,76,77,78,80,81</sup> the theoretical description of hard-core liquid crystals and have come up with quite simple models that do in fact predict smectic and, in some cases, columnar phases.

## 7.2. The Effect of Rotation

Of course, a model system consisting of *parallel* spherocylinders is rather unphysical. It is therefore of considerable interest to know whether if a system of freely rotating hard-core molecules can form a smectic phase. This question is of some practical interest, in view of the recent experimental evidence that smectic<sup>82</sup> and columnar<sup>83</sup> ordering may take place in concentrated solutions of rod-like DNA molecules.

Simulations<sup>84,85</sup> of a system of freely rotating spherocylinders with length-to-width ratio  $L/D = 5$  revealed the presence of a stable smectic phase, in addition to the expected isotropic, nematic and solid phases. This work was recently extended to other aspect ratios by Veerman and Frenkel<sup>86</sup>. These authors show that the smectic phase disappears at  $L/D = 3$ . At this aspect ratio, the nematic phase is no longer (meta-)stable. Fig. 8 shows a tentative phase diagram of freely rotating hard spherocylinders.

Density-functional theories for hard spherocylinder systems have been proposed by Holyst and Poniewierski<sup>76,77</sup> and by Somoza and Tarazona<sup>87,88</sup>. Both theories predict the presence of a stable smectic phase if the length-to-width ratio  $L/D$  exceeds a minimum value of  $\sim 3$ . However, the two theories differ in their estimate of the point where the nematic-smectic transition has its tricritical point.

## 7.3. Columnar Phases

If hard-core models exhibit smectic phases, one may wonder if excluded volume effects can also induce the formation of the even more ordered columnar phase. In this case, it is natural to look for a convex, plate-like molecule. Oblate ellipsoids are not expected to form columnar phases. The argument why this should be so is essentially the same as the one that 'explains' why prolate ellipsoids should not form smectic phases. Rather, we should look for the oblate equivalent of the spherocylinder.

For ellipsoids the transition from prolate to oblate shapes is controlled by a single parameter (the axial ratio  $a/b$ ). In contrast, spherocylinders cannot be changed into oblate particles simply by changing  $L/D$  (unless we allow for the possibility of negative  $L/D$ ). It turns out that a particularly convenient 'oblate spherocylinder' model is the so-called *cut sphere*<sup>89</sup> (see Fig. 9).

The cut sphere is a hard convex body. Using the standard techniques applicable to such objects (see e.g. Ref. 90), the second virial coefficient of cut spheres can be evaluated for arbitrary  $L/D$  ratios:

$$B_2 = \frac{\pi D^3}{6} \left\{ \cos \theta_M \left( 1 + \frac{\sin^2 \theta_M}{2} \right) + 3 \left( \cos \theta_M + \frac{\theta_M \sin \theta_M}{2} \right) \left( \cos \theta_M + \frac{\sin^2 \theta_M}{2} \right) \right\} \quad (23)$$

where  $\theta_M \equiv \arccos(L/D)$ .

At high densities, cut spheres can be stacked in a regular close-packed lattice. The volume fraction at regular close-packing is:  $\eta_{cp} = (\pi/6)\sqrt{3 - (L/D)^2}$ . Note that for  $L/D = 1$  (hard spheres), this reduces to the well-known hard-sphere result  $\eta_{cp} = \pi/\sqrt{18}$ . For  $L/D \rightarrow 0$  (flat, cylindrical platelets), we obtain the  $2D$  hard-disk value  $\eta_{cp} = \pi/\sqrt{12}$ . Monte Carlo simulations were carried out on a system of cut spheres with  $L/D = 0.1$  and  $L/D = 0.2$ , over a range of densities between dilute gas and crystalline solid<sup>89,91</sup>. Surprisingly, it turned out that the systems with  $L/D = 0.1$  and  $L/D = 0.2$  behaved completely differently.

For the system with  $L/D = 0.1$  it was observed that the system spontaneously ordered to form a nematic phase at a reduced density of 0.335 (i.e. at 33.5% of regular close packing). At a density corresponding to 49% of regular close packing, this nematic phase undergoes a strong first-order transition to a columnar phase (at a reduced density  $\rho^* = 0.534$ ). The columnar-crystalline transition occurs at much higher density ( $\rho^* > 0.80$ ).

Next, we turn to the system of platelets with  $L/D = 0.2$ . At first sight, the behavior of this system looks quite similar to that observed for the thinner platelets. In particular, the equation-of-state for cut spheres with  $L/D = 0.2$  looks similar to the one corresponding to  $L/D = 0.1$ . At low densities the compressibility factor is well described by a 5-term virial series and at higher densities the actual pressure is lower. In other hard-core systems this is usually an indication of a precursor to some kind of ordering transition (e.g. the I-N transition in the  $L/D = 0.1$  case). And, indeed, at  $\rho \approx 0.475$  a change of slope in the equation of state, as is to be expected in a simulation near a weakly first-order (or, possibly, second-order) phase transition. The most natural assumption is that an isotropic-nematic transition takes place. After all, this is what happens in the  $L/D = 0.1$  case, and we also know that oblate hard ellipsoids with a axial

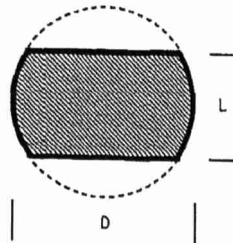


Fig.9. Schematic drawing of the cut-sphere model. This model is used as an oblate counterpart of the hard spherocylinder model.

ratio less than 0.4 have a stable nematic phase. However, if we measure the orientational correlation function  $g_2(r) \equiv \langle P_2(\mathbf{u}(0) \cdot \mathbf{u}(r)) \rangle$  we find that it decays to zero within one molecular diameter, even at the highest densities of the 'fluid' branch (see Fig. 10). In a nematic phase,  $g_2(r)$  should tend to a finite limit:  $g_2(r) \rightarrow S^2$  as  $r \rightarrow \infty$ , where  $S$  is the nematic order parameter.

It should be stressed that the absence of nematic order in the  $L/D = 0.2$  system is not a consequence of the way in which the system was prepared. Even if we started with a configuration at a reduced density  $\rho/\rho_{cp} = 0.50$  with all the molecules initially aligned, the nematic order would rapidly disappear. In other words, at that density the nematic phase is *mechanically* unstable.

The great surprise comes when we consider the higher-order orientational correlation function  $g_4(r) \equiv \langle P_4(\mathbf{u}(0) \cdot \mathbf{u}(r)) \rangle$ . Usually, when  $g_2(r)$  is short ranged, the same holds *a fortiori* for  $g_4(r)$ . However, Fig. 11 shows that for densities  $\rho/\rho_{cp} > 0.55$ ,  $g_4(r)$  is much longer ranged than  $g_2(r)$ . This suggests that the system has a strong tendency towards orientational order with *cubic* symmetry (we reserve the term 'cubatic' for a phase with cubic orientational order but no translational order. In contrast, 'cubic' is used to denote a phase with cubic translational order). In computer simulations one should always be very suspicious of any spontaneous ordering with cubic symmetry, because such ordering could be induced by the (cubic) periodic boundary conditions.

In order to test whether the boundary conditions were responsible for the cubatic order we did a number of long simulations with systems of up to 2048 particles. These simulations strongly suggest that the onset of cubatic orientational order is not an artifact of the boundary conditions. Another indication that the boundary conditions are not the cause of the observed ordering is that still higher order correlations ( $g_6$  and  $g_8$ ) that could also be induced by the periodic boundaries, are in fact rapidly decaying functions of  $r$ . If we make a log-log plot of  $g_4(r)$  in the large system for several densities between  $\rho = 0.51$  and  $\rho = 0.63$  (see Fig. 12), it appears that the cubatic order is not truly long-ranged but quasi-long-ranged, i.e.  $g_4(r) \sim r^{-\eta}$ , where  $\eta$  depends on the density  $\rho$ . This observation should, however, be taken with a large grain of salt, as the range over which

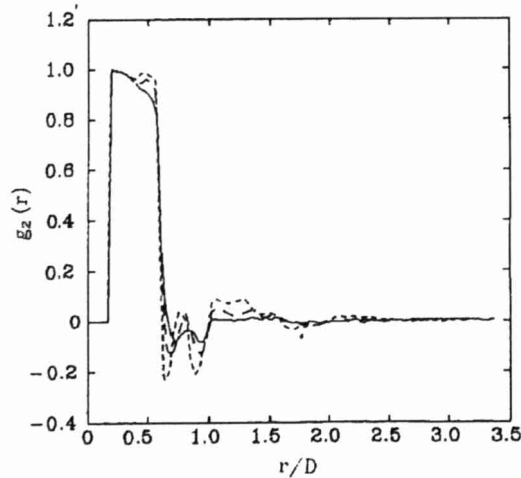


Fig. 10. Density dependence of the orientational correlation function  $g_2 \equiv \langle P_2(\mathbf{u}(0) \cdot \mathbf{u}(r)) \rangle$  in a system of hard cut spheres with a lengthtowidth ratio  $L/D = 0.2$ . Drawn curve:  $\rho/\rho_{cp} = 0.51$ , long dashes:  $\rho/\rho_{cp} = 0.57$ , short dashes:  $\rho/\rho_{cp} = 0.51$ , dotted:  $\rho/\rho_{cp} = 0.63$ . Note that even at the highest densities studied  $g_2(r)$  is short ranged.

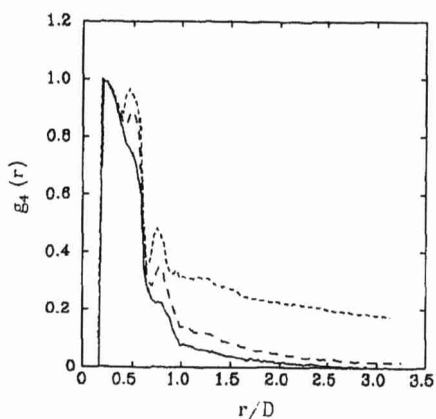


Fig.11. Density dependence of the orientational correlation function  $g_4 = \langle P_2(\mathbf{u}(0) \cdot \mathbf{u}(r)) \rangle$  in a system of hard cut spheres with a length-to-width ratio  $L/D=0.2$ . Symbols as in Fig. 10. Note that, unlike  $g_2(r)$ ,  $g_4(r)$  appears to be long-ranged at high densities.

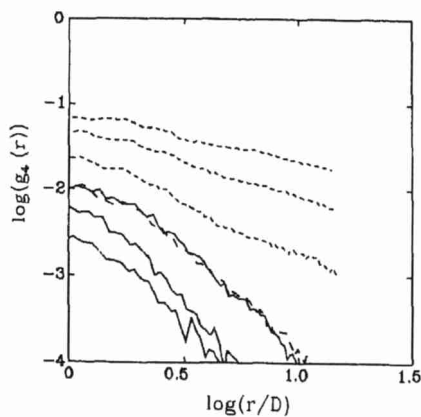


Fig.12. Log-log plot of the orientational correlation function  $g_4 = \langle P_2(\mathbf{u}(0) \cdot \mathbf{u}(r)) \rangle$  in a system of hard cut spheres with a length-to-width ratio  $L/D=0.2$  as a function of density. With increasing density, the amplitude of this correlation function increases. The lowest curve corresponds to  $\rho^* = 0.51$ , followed by curves for  $\rho^* = 0.54$  and  $\rho^* = 0.56$ . The long-dashed curve corresponds to  $\rho^* = 0.57$ . At higher densities  $\rho^* = 0.58, 0.60$  and  $0.63$  (long-dashed curves),  $g_4(r)$  appears to decay algebraically over the narrow range of distances ( $1 < r/D < 3.2$ ) where we could observe monotonic decay of  $g_4(r)$ .

linear behavior in the loglog plot is observed corresponds to less than 1 decade in  $r$ .

Simulations by Veerman<sup>91</sup> indicate that, at least for the model with  $L/D = 0.2$ , the cubatic phase may be largely meta-stable. This observation does not diminish the interest of this phase. After all, many liquid-crystalline phases that occur in nature are only metastable, but still very real. I am, however, not aware of any experimental observations of *cubatic* liquid crystals, although *cubic* liquid-crystalline phase of disklike molecules have been observed experimentally<sup>92</sup>.

## 8. Conclusion

In this review, I have almost exclusively discussed phase transitions in hard-core models. However, I do not wish to suggest that excluded volume effects are the whole story. On the contrary, such models provide only a moderately realistic description of some lyotropic liquid crystals, and they are totally unrealistic for thermotropic liquid crystals. It is therefore of crucial importance to investigate the effect of longer-ranged attractive forces and of molecular flexibility on the stability of liquid crystalline phases. The recent work of Rull et.al.<sup>68</sup> shows clearly that attraction can have a drastic effect on the stability of liquid-crystalline phases in simple model systems. Most importantly, the results of Ref. 68 suggest that thermodynamic perturbation theory may be much less successful for liquid-crystalline phases than for simple liquids. If so, this would imply that we may have to revise the concept of a hard-core reference system for a liquid crystal.

Thus far, there have been no direct numerical studies of the location of phase-transitions involving meso-phases of flexible molecules. As was explained in the beginning of this paper, the reason is simply that simulations of flexible molecules are quite time-consuming. However, this situation is likely to change due to recent advances in the simulation of flexible molecules<sup>93,94,95</sup>. Once we can perform efficient simulations flexible mesogens, it becomes possible to connect the numerical study of simple mesogens with that of liquid-crystalline polymers and of ordering in self-assembling structures.

**ACKNOWLEDGMENTS.** The work of the FOM Institute is part of the research program of FOM and is made possible with financial help from the Nederlandse Organisatie voor Wetenschappelijk Onderzoek (NWO). Part of the work reported in this paper was carried out at the FOM Institute by Jan Veerman and Jose Cuesta. I thank both for their assistance in preparing some of the illustrations in this paper. I thank Mike Allen for permission to reproduce Fig. 2.

## References

1. M.P. Allen and D.J. Tildesley, "Computer Simulation of Liquids", Clarendon, Oxford, 1987.
2. N. Metropolis, A.W. Rosenbluth, M.N. Rosenbluth, A.H. Teller and E. Teller, J. Chem. Phys. **21**: 1087 (1953).
3. M. Parrinello and A. Rahman, Phys. Rev. Lett. **45**: 1196 (1980).
4. M. Parrinello and A. Rahman, J. Appl. Phys. **52**: 7182 (1981).
5. R. Najafabadi and S. Yip, Scripta Metall. **17**: 1199 (1983).
6. M.J. Mandell, J. Stat. Phys. **15**: 299 (1976).
7. P.J. Steinhardt, D.R. Nelson and M. Ronchetti, Phys. Rev. B **28**: 784 (1983).
8. R.W. Impey, P.A. Madden and D.J. Tildesley, Mol. Phys. **44**: 1319 (1981).
9. M. Fixman, Proc. Nat. Acad. Sci. **71**: 3050 (1974).
10. L. Verlet, Phys. Rev. **159**: 98 (1967).
11. H.J.C. Berendsen and W.F. van Gunsteren, in: "Molecular Dynamics Simulations of Statistical Mechanical Systems", Proceedings of the 97th International School of Physics 'Enrico Fermi', G. Ciccotti and W. G. Hoover, editors. NorthHolland, Amsterdam, 1985, p.43.

12. M.P. Allen, D. Frenkel and J. Talbot, *Computer Physics Reports* **9**: 301 (1989).
13. J.J. Erpenbeck and W.W. Wood in: "Statistical Mechanics", Part B, ed. B.J. Berne, Plenum Press, New York, 1977.
14. J.L. Lebowitz, J.K. Percus and L. Verlet, *Phys. Rev.* **153**: 250 (1967).
15. H.C. Andersen, *J. Chem. Phys.* **72**: 2384 (1980).
16. S. Nose, *J. Chem. Phys.* **81**: 511 (1984).
17. W.W. Wood, *J. Chem. Phys.* **48**: 415 (1968).
18. I.R. McDonald, *Mol. Phys.* **23**: 41 (1972).
19. G.E. Norman and V.S. Filinov, *High Temp. Res. USSR* **7**: 216 (1969).
20. D.J. Adams, *Mol. Phys.* **28**: 1241 (1974).
21. M. Creutz, *Phys. Rev. Lett.* **50**: 1411 (1983).
22. A. Panagiotopoulos, *Mol. Phys.* **61**: 813 (1987).
23. G. Ciccotti, D. Frenkel and I.R. McDonald, "Simulation of Liquids and Solids", NorthHolland, Amsterdam, 1987. This reprint collection contains, among others, Ref.s 2, 4, 14, 15, 16, 18, 10, 24, 28.
24. R. Zwanzig and N.K. Ailawadi, *Phys. Rev.* **182**: 280 (1969).
25. D. Frenkel in: "Intermolecular Spectroscopy and Dynamical Properties of Dense Systems", Proceedings of the 75th International School of Physics 'Enrico Fermi', J. van Kranendonk, ed., Soc. Italiana di Fisica, Bologna, 1980, p.156.
26. G. Jacucci and A. Rahman, *Nuovo Cimento D* **4**: 341 (1984).
27. D. Frenkel in: "Molecular Dynamics Simulations of Statistical Mechanical Systems", Proceedings of the 97th International School of Physics 'Enrico Fermi', G. Ciccotti and W. G. Hoover, editors. NorthHolland, Amsterdam, 1985, p.151.
28. W.G. Hoover and F.H. Ree, *J. Chem. Phys.* **47**: 4873 (1967).
29. J.P. Hansen and I.R. McDonald, "Theory of Simple Liquids", 2nd edition, Academic Press, London, 1986.
30. E.J. Meijer, D. Frenkel, R.A. LeSar and A.J.C. Ladd, *J. Chem. Phys.* **92**: 7570 (1990).
31. D. Frenkel and B.M. Mulder, *Mol. Phys.* **55**: 1171 (1985).
32. W.G.T. Kranendonk and D. Frenkel, *Mol. Phys.* **72**: 699 (1991).
33. P.G. de Gennes, "Physics of Liquid Crystals", Oxford University Press, Oxford, England (1974).
34. L. Onsager, *Proc. NY. Acad. Sci.* **51**: 627 (1949).
35. W. Maier and A. Saupe, *Z. Naturforsch. A* **13**: 564 (1958).
36. F. Dowell and D.E. Martire, *J. Chem. Phys.* **68**: 1088(1978), *ibid.*: **68**: 1094 (1978), *ibid.*: **69**: 2322 (1978). F. Dowell, *Phys. Rev. A* **28**: 3526 (1983).
37. W.M. Gelbart and A. Gelbart, *Mol. Phys.* **33**: 1387 (1977).
38. B.J. Alder and T.E. Wainwright, *J. Chem. Phys.* **27**: 1208 (1957).
39. J.D. Weeks, D. Chandler and H.C. Andersen, *J. Chem. Phys.* **54**: 5237 (1971).
40. See, for instance: C. Zannoni in "The molecular physics of liquid crystals", G.R. Luckhurst and G.W. Gray editors, Academic Press, London, 1979, p.191.
41. P.A. Lebowitz and G. Lasher, *Phys. Rev. A* **6**: 426 (1972).
42. J. Vieillard-Baron, *J. Chem. Phys.* **56**: 4729 (1972).
43. J. Vieillard-Baron, *Mol. Phys.* **28**: 809 (1974).
44. W.G. Hoover and F.H. Ree, *J. Chem. Phys.* **49**: 3609 (1968).
45. R. Eppenga and D. Frenkel, *Mol. Phys.* **52**: 1303 (1984).
46. M.P. Allen and M.R. Wilson, *J. Computer-Aided Molec. Design* **3**: 335 (1989).
47. D. Frenkel, *Mol. Phys.* **54**: 145 (1985).
48. M.P. Allen, *Liquid Crystals*, **8**: 499 (1990).
49. B.M. Mulder, *Phys. Rev. A* **39**: 360 (1989), *Liquid Crystals* **8**: 527 (1990).
50. M.A. Cotter and D.E. Martire, *J. Chem. Phys.* **52**: 1902 (1970), *J. Chem. Phys.* **53**: 4500 (1970).
51. M.A. Cotter, *Phys. Rev. A* **10**: 625 (1974), *J. Chem. Phys.* **66**: 1098 (1977).
52. B. Barboj and W.M. Gelbart, *J. Chem. Phys.* **71**: 3053 (1979).  
B. Barboj and W.M. Gelbart, *J. Stat. Phys.* **22**: 685 (1980).
53. B.M. Mulder and D. Frenkel, *Mol. Phys.* **55**: 1193 (1985).
54. U.P. Singh and Y. Singh, *Phys. Rev. A* **33**: 2725 (1986).
55. M. Baus, J.L. Colot, X.G. Wu and H. Xu, *Phys. Rev. Lett.* **59**: 2148 (1987).
56. J.F. Marko, *Phys. Rev. Lett.* **60**: 325 (1989). J.F. Marko, *Phys. Rev. A* **39**: 2050 (1989).
57. J.L. Colot, X.G. Wu, H. Xu and M. Baus, *Phys. Rev. A* **38**: 2022 (1988).
58. A. Perera, P.G. Kusalik and G.N. Patey, *J. Chem. Phys.* **87**: 1295 (1987), **89**: 5969(1988). A. Perera, G.N. Patey and J.J. Weis, *J. Chem. Phys.* **89**: 6941 (1989). A. Perera and G. N. Patey, *J. Chem. Phys.* **89**: 5861 (1989).

59. J.M. Kosterlitz and D. Thouless, *J. Phys.* **C6**: 1181 (1973).
60. M. Romeiro, *J. Math. Phys.* **19**: 802 (1978).
61. D. Frenkel and R. Eppenga, *Phys. Rev. A* **31**: 1776 (1985).
62. R.F. Kayser and H.J. Raveche, *Phys. Rev. A* **17**: 2067 (1978).
63. J.A. Cuesta, C.F. Tejero and M. Baus, *Phys. Rev. A* **39**: 6498 (1989).
64. J.A. Cuesta and D. Frenkel, *Phys. Rev. A* **42**: 2126 (1990).
65. M.J.P. Gingras, P.C.W. Holdsworth and B. Bergersen, in "Proceedings of the 13th International Liquid Crystal Conference" (in press), and M.J.P. Gingras, P.C.W. Holdsworth and B. Bergersen, *Phys. Rev. A* **41**: 6786 (1990).
66. M. Hosino, H. Nakano and H. Kimura, *J. Phys. Soc. Japan* **46**: 1709 (1979).
67. Recently, it has been shown that this argument does not extend to models that include attractive forces. In particular, it has been shown that the Gay-Berne model, i.e. the 'ellipsoidal' generalization of the Lennard-Jones model for atomic fluids, does indeed exhibit one or more stable smectic phases<sup>68</sup>.
68. E. de Miguel, L.F. Rull, M.K. Chalam, K.E. Gubbins and F. van Swol, *Mol. Phys.* **72**: 593 (1991).
69. A. Stroobants, H.N.W. Lekkerkerker and D. Frenkel, *Phys. Rev. Lett.* **57**: 1452 (1986).
70. A. Stroobants, H.N.W. Lekkerkerker and D. Frenkel, *Phys. Rev. A* **36**: 2929 (1987).
71. J.A.C. Veerman, thesis, University of Utrecht, 1991. J.A.C. Veerman and D. Frenkel, *Phys. Rev. A* (in press).
72. B.M. Mulder, *Phys. Rev. A* **35**: 3095 (1987).
73. X. Wen and R.B. Meyer, *Phys. Rev. Lett.* **59**: 1325 (1987).
74. A.M. Somoza and P. Tarazona, *Phys. Rev. Lett.* **61**: 2566 (1988).
75. R. Holyst and A. Poniewierski, *Phys. Rev.* **39**: 2742 (1988).
76. A. Poniewierski and R. Holyst, *Phys. Rev. Lett.* **61**: 2461 (1988).
77. R. Holyst and A. Poniewierski, preprint.
78. M.P. Taylor, R. Hentschke and J. Herzfeld, *Phys. Rev. Lett.* **62**: 800 (1989), *ibid*: **62**: 1577 (1989).
79. M.P. Taylor, R. Hentschke and J. Herzfeld, *Phys. Rev. A* **40**: 1678 (1989).
80. J.M. Caillol and J.J. Weis, *J. Chem. Phys.* **90**: 7403 (1989).
81. T.J. Sluckin, *Liquid Crystals* **6**: 111 (1989).
82. T.E. Strzelecka, M.W. Davidson and R.L. Rill, *Nature*, **331**: 457 (1988).
83. F. Livolant, A.M. Levelut, J. Doucet and J.P. Benoit, *Nature* **339**: 724 (1989).
84. D. Frenkel, *J. Phys. Chem.* **92**: 3280 (1988).
85. D. Frenkel, H.N.W. Lekkerkerker and A. Stroobants, *Nature* **332**: 822 (1988).
86. J.A.C. Veerman and D. Frenkel, *Phys. Rev. A* **41**: 3237 (1990).
87. A.M. Somoza and P. Tarazona, *Phys. Rev. A* **41**: 965 (1990).
88. A.M. Somoza and P. Tarazona, *J. Chem. Phys.* **91**: 517 (1989).
89. D. Frenkel, *Liquid Crystals*, **5**: 929 (1989).
90. T. Boublik and I. Nezbeda, *Coll. Czechoslovak. Chem. Commun.* **51**: 2301 (1986).
91. J.A.C. Veerman, thesis, University of Utrecht, 1991. J.A.C. Veerman and D. Frenkel, to be published.
92. J. Billart, *C.R. Acad. Sci. Paris*, **305**: 843 (1987).
93. J.I. Siepmann, *Mol. Phys.* **70**: 1145 (1990).
94. D. Frenkel, *J. Phys. Condensed Matter* **2(SA)**: 265 (1990).
95. D. Frenkel, *Physica A*, submitted for publication.